JOURNAL OF ENVIRONMENTAL SCIENCES 124 (2023) 19–30

Available online at www.sciencedirect.com

ScienceDirect

www.elsevier.com/locate/jes

JES JOURNAL OF ENVIRONMENTAL SCIENCES

www.jesc.ac.cn

Spatial distribution of fossil fuel derived CO_2 over India using radiocarbon measurements in crop plants

Rajveer Sharma[1,2,*], *Ravi Kumar Kunchala*[2,*], *Sunil Ojha*[1], *Pankaj Kumar*[1], *Satinath Gargari*[1], *Sundeep Chopra*[1]

[1] *Inter University Accelerator Centre, New Delhi 110067, India*

[2] *Centre for Atmospheric Sciences, Indian Institute of Technology Delhi, New Delhi 110016, India*

ARTICLE INFO

Article history:
Received 13 July 2021
Revised 23 October 2021
Accepted 2 November 2021
Available online 1 February 2022

Keywords:
Carbon dioxide
Crop plants
Fossil fuel CO_2
Radiocarbon measurements

ABSTRACT

Examining the contribution of fossil fuel CO_2 to the total CO_2 changes in the atmosphere is of primary concern due to its alarming levels of fossil fuel emissions over the globe, specifically developing countries. Atmospheric radiocarbon represents an important observational constraint and utilized to trace fossil fuel derived CO_2 (CO_{2ff}) in the atmosphere. For the first time, we have presented a detailed analysis on the spatial distribution of fossil fuel derived CO_2 (CO_{2ff}) over India using radiocarbon ($\Delta^{14}C$) measurements during three-year period. Analysis shows that the $\Delta^{14}C$ values are varying between 29.33‰ to -34.06‰ across India in the year 2017, where highest value belongs to a location from Gujarat while lowest value belongs to a location from Chhattisgarh. Based on the $\Delta^{14}C$ patterns, spatial distributions of CO_{2ff} mole fractions have been determined over India and the calculated values of CO_{2ff} mole fractions are varying between 4.85 ppm to 26.59 ppm across India. It is also noticed that the highest CO_{2ff} mole fraction is observed as 26.59 ppm from a site in Chhattisgarh. CO_{2ff} mole fraction values from four high altitude sites are found to be varied between 4.85 ppm to 14.87 ppm. Effect of sampling different crop plants from the same growing season and different crop plant organs (grains, leaves, stems) on the $\Delta^{14}C$ and CO_{2ff} have been studied. Annual and intra seasonal variations in the $\Delta^{14}C$ and CO_{2ff} mole fractions have also been analyzed from a rural location (Dholpur, Rajasthan).

Introduction

Atmospheric carbon dioxide (CO_2) has been identified to be the most important anthropogenic greenhouse gas (GHG) responsible for the cause of global warming (Stocker et al., 2013). CO_2 has been rising rapidly over the globe since the industrial revolution and has now reached dangerous levels due to increase in anthropogenic activities (Le Quéré et al., 2013; Van De Wal et al., 2011). This alarming increase in CO_2 in the atmosphere has significantly influenced the radiative forcing of the planet (Boesch et al., 2011; Stocker et al., 2013). CO_2 exchanges rapidly with the other reservoirs: the oceans, land and terrestrial biosphere. Terrestrial biosphere absorbs CO_2 during the photosynthesis process of plants and releases it by the respiration process from living organisms and soil. Terrestrial

* Corresponding authors.
E-mails: rajveersharma1988@gmail.com (R. Sharma), rkkunchala@cas.iitd.ac.in (R.K. Kunchala).

https://doi.org/10.1016/j.jes.2021.11.003
1001-0742/

biosphere acts as a source of CO_2 during respiration and sink during photosynthesis (Prentice et al., 2001; Trumbore, 2006). Similarly, oceans act as a sink when their upwelling water is low in CO_2 and act as a source when their upwelling water is rich in CO_2 (Turnbull et. al., 2016a). In these natural exchanges, net flux of CO_2 remains roughly constant over an annual and decadal time scales (Metya et al., 2021; Turnbull et. al., 2016a). This natural balance of CO_2 is perturbed after industrialization when a high amount of CO_2 is added into the atmosphere because of anthropogenic activities, mainly combustion of fossil fuels (Ciais et al., 2013). The additional CO_2 flux added into the atmosphere is not in balance with natural CO_2 flux (Turnbull et al., 2016a). Therefore, this leads to continuous increases in the levels of atmospheric CO_2 and its value reaches up to 410.5 ppm in 2019, which resulted in an increase of 148% to that of pre-industrial levels (278 ppm) (WMO, 2020). To make mitigation policies for the reduction of CO_2, and also to understand the future climate, it is crucial to examine the exact contribution of CO_2 from fossil fuel combustion.

After China and the US, India is the third largest emitter of CO_2 in the world since 2010 (Lin et al., 2015). CO_2 emissions have been increased by 5.1% per year for the past ten year time period from 2009 to 2018 in India (Friedlingstein et al., 2019). Estimates of CO_2 budget from India based on either bottom-up approach or top-down approach poses larger uncertainties (100-150%). One of the reasons for the uncertainties of these estimations is the unavailability of sufficient spatial and temporal ground-based observational data in India (Lin et al., 2015). The sparseness of the observational data is the biggest constraint for accurately estimating the fossil fuel derived CO_2 emissions from India. In the recent decade, a few ground-based observations stations have been established in western India and the Himalayas to monitor atmospheric CO_2 and other greenhouse gases (GHG), located at Sinhagad (18.35°N, 73.75°E, 1600m a.s.l.; Kumar et al., 2014; Tiwari et al., 2014), Mount Abu (24.60°N, 72.70°E, 1700 m a.s.l.), Ahmedabad (23.00°N, 72.50°E, 55 m a.s.l.; Lal et al., 2015), Nainital (29.37°N, 79.45°E, 1958 m a.s.l.; Kumar et al., 2010) and Darjeeling (27.03°N, 88.15°E, 2194 m a.s.l.; Ganesan et al., 2013). With the existing ground-based observations, few studies have been carried out over Indian sub-continent to address the variations of atmospheric CO_2 and other GHGs (Tiwari et al., 2011, 2013, 2014; Lin et al., 2015; Chandra et al., 2016). Most of these studies are mainly addressed the spatiotemporal variations of surface CO_2 and GHGs over the study region. These ground-based observations are very much essential to address the sources and sinks of CO_2 through inversion approach. Studies also highlighted on the uncertainties in the estimations of fossil fuel CO_2 due to sparsity of ground-based observations over Indian region (Patra et al., 2013; Swathi et al., 2013). Although, estimation of fossil fuel derived CO_2 (CO_{2ff}) based on the observations of CO_2 alone is difficult because CO_{2ff} is distributed between different reservoirs such as atmosphere, biosphere and oceans which results in large uncertainties in the flux calculations from each reservoir. Also another difficult part is the separation of CO_{2ff} signal from the other sources too. Therefore, the best and direct way to separate CO_{2ff} signal from other sources is to measure the radiocarbon content of atmospheric CO_2 (Turnbull et al., 2006).

Traditionally, fossil fuel contributions are calculated based on the bottom-up approach. In this approach, energy statistics data and emission factors are used for the estimation of fossil fuel derived CO_2 (CO_{2ff}). However, this method has large uncertainties up to 50% (Marland et al., 2003; Andres et al., 2012). An alternative method to verify bottom-up estimates is to use atmospheric tracers such as ^{14}C, CO and SF_6 (Turnbull et al., 2006). Radiocarbon (^{14}C, half-life of 5730 years) is the best tracer for the estimation of fossil fuel CO_2 (CO_{2ff}) because fossil fuels do not contain radiocarbon. When CO_2, produced by burning of fossil fuels, is mixed with atmospheric CO_2, it dilutes the $^{14}C/^{12}C$ ratio. This effect is known as the Suess effect (Suess, 1955). CO_2 emitted by volcanoes and upwelling water from deep ocean is also depleted in ^{14}C and can dilute $^{14}C/^{12}C$ ratio (Turnbull et al., 2016a) in addition to the fossil fuels. The dilution effect of CO_2 from volcano is visible only within 1 km range of volcanic activity (Turnbull et al., 2016a) and dilution effect of CO_2 from deep ocean is more pronounced in southern hemisphere (Levin and Hesshaimer, 2000). On the other hand, in northern hemisphere, various studies reported that the fossil fuels are the primary reason for the declination of $^{14}C/^{12}C$ ratio (Randerson et al., 2002; Levin et al., 2003; Turnbull et al., 2006; Hsueh et al., 2007). Dilution in the $^{14}C/^{12}C$ ratio is (represented by $\Delta^{14}C$) utilized to determine the mole fraction of fossil fuel derived CO_2 (CO_{2ff}). Radiocarbon content (in terms of $\Delta^{14}C$) of atmospheric CO_2 can be determined either by collecting atmospheric air samples in flasks or using passive absorption of CO_2 over NaOH statically or using a pump. These methods are the best suitable for studying the temporal variations in the radiocarbon content in the atmosphere at any geographical location (Turnbull et. al., 2007, 2016b, 2017; Levin et. al., 2003; Wenger et al, 2019). But it is difficult to use these sample collection methods for finding out the spatial distribution over a large area (Bozhinova et al., 2013). Leaves of annual crop plants or deciduous trees can also be used for this purpose (Hsueh et al., 2007; Bozhinova et al., 2013, 2016; Varga et al., 2020; Niu et al., 2016). Plants leaves assimilate atmospheric CO_2 during photosynthesis (day time) and utilize it for plant growth. Thus, radiocarbon measurement of crop plants can provide a time-integrated signature of fossil fuel CO_2 for the duration of plant growth period. Although, in the interpretation of this signal from plant samples, local environment, choice of crop plant and plant organ also play an important role (Bozhinova et al., 2013).

To keep the limitations and constraints of observational data on understanding the aforesaid estimations, the present study provides a detailed examination on the CO_{2ff} using the radiocarbon measurements over different locations in India for three-year time period (2017, 2018 and 2020). For the first time, to the best of our knowledge, we have examined the spatial variations of fossil fuel derived CO_2 across India by measuring radiocarbon in crop plants. Moreover, our study is focused on understanding the following points in detail: (1) determination of the spatial distribution of $\Delta^{14}C$ across India, (2) determination of the spatial distribution of CO_{2ff} over Indian region, (3) studying the effect of sampling of different plant organs and crop plants on the $\Delta^{14}C$ and CO_{2ff} values, (4) studying the annual and intra seasonal variations in $\Delta^{14}C$ and CO_{2ff} values from a single location.

1. Material and methods

1.1. Sampling locations and sample collection

In the present study, we have collected fully mature wheat plants for the analysis. If a full plant is not available, then we have collected leaves, grains and stem as well. Wheat crop is grown in the winter season (also called rabi season, October – November to March – April) of north India (DES, 2015). Growing period of wheat varies with the local environmental and climatic conditions. It is also known that over some parts of the country, this period starts little earlier (September-October to February-March) while other parts happen to be little later (November -December to April-May) (DES, 2015). Also, in some parts of the country, where we could not get wheat, we have collected other crop plants grown in the same period such as mustard (leaves and grains), rice paddies, barely grains as well. All the samples were collected from the 29 locations across India for the years 2017 (21 locations), 2018 (5 locations) and 2020 (3 locations). Over some locations, different types of crop plants (wheat, rice, mustard etc.) were also collected to study the effect of sampling different crop plants on $\Delta^{14}C$ and CO_{2ff} values. In addition to the above samples, we also collected samples from a rural location (Dholpur, Rajasthan) for three year time period i.e., 2017, 2018 and 2020, respectively. All the details about the sampling locations (latitude and longitude) including the year of sampling have been described in detail in the supplementary data. We have taken care to avoid the effect of local pollution, therefore these samples were collected from locations those are far from residential areas, highways and paved roads. In addition to the samples collected as per above criteria, we have also collected some samples from the roadside to see the contribution of local fossil fuel sources in CO_{2ff}.

1.2. Sample pretreatment, graphitization and radiocarbon measurement

Samples were first dried at 50°C overnight and then treated with 0.5 mol/L HCl acid for 1 hr to remove any carbonate and other extraneous carbon. After acid treatment, samples were rinsed 5–6 times up to neutralization of pH and then samples were dried in the freeze dryer overnight. Sufficient amounts (that can produce 1 mg C) of dried samples were packed into tin boats and combusted in elemental analyzer and produced CO_2 was graphitized using automated graphitization equipment (AGE) in the graphitization laboratory of Accelerator Mass Spectrometry (AMS) facility at Inter University Accelerator Centre (IUAC), New Delhi (Sharma et al., 2019). Graphite produced from the samples were packed into aluminum target holders and measured using XCAMS (the ^{14}C Compact Accelerator Mass Spectrometer eXtended for ^{10}Be and ^{26}Al) with primary standards (OXII), secondary standards and background samples with precision less than 3‰.

1.3. Calculation of $\Delta^{14}C$

$^{14}C/^{12}C$ ratios measured using XCAMS system were converted into $\Delta^{14}C$ using the following relation (Stuiver and Polach, 1977):

$$\Delta^{14}C = \left[\frac{\left(\frac{^{14}C}{^{12}C}\right)_{SN}}{\left(\frac{^{14}C}{^{12}C}\right)_{abs}} - 1\right] X\ 1000\% \quad (1)$$

where $(^{14}C/^{12}C)_{SN}$ is the $^{14}C/^{12}C$ ratio of the samples normalized to a constant value of delta ^{13}C of -25‰ and $(^{14}C/^{12}C)_{abs}$ is the absolute ratio of radiocarbon reference standard corrected for fractionation and radiocarbon decay. Uncertainties in the $\Delta^{14}C$ values for individual samples are based on the uncertainties in the measured $^{14}C/^{12}C$ ratio. Uncertainties in the $^{14}C/^{12}C$ ratio are purely based on the counting statistics and calculated in the following way: as a first step, uncertainties of unknown sample and background sample are added in quadrature, square root is calculated and relative uncertainty is calculated after dividing it with background subtracted ratio. In the second step, relative uncertainty of background-subtracted ratio is added in quadrature with relative uncertainty of standard sample and final uncertainty is calculated after taking the square root of this sum and multiplied it with corresponding percent modern carbon (pMC) value. All the samples in this study are measured in several cathode wheels in XCAMS from the year 2018 to 2020. An external uncertainty of 3.71‰ is estimated by taking standard deviation of mean of 20 IAEA C3 samples measured in all these wheels.

1.4. Calculation of CO_{2ff}

Measured mole fraction of CO_2 at any location can be assumed of CO_2 from a clean air background site (CO_{2bg}), fossil fuel sources (CO_{2ff}) and CO_2 from other sources (CO_{2oth}) such as heterotopic respiration, nuclear power plants and oceans. According to mass balance equation (Levin et al., 2003)

$$CO_{2mes} = CO_{2bg} + CO_{2ff} + CO_{2oth} \quad (2)$$

Similarly, $\Delta^{14}C$ measured at any location ($\Delta^{14}C_{mes}$) can also be represented using isotopic mass balance in following way

$$\Delta^{14}C_{mes}(CO_{2mes}) = \Delta^{14}C_{bg}CO_{2bg} + \Delta^{14}C_{ff}CO_{2ff} + \Delta^{14}C_{oth}CO_{2oth} \quad (3)$$

where, $\Delta^{14}C_{mes} = \Delta^{14}C$ measured in the crop plants in this study

$\Delta^{14}C_{bg} = \Delta^{14}C$ measured at clean air background site

$\Delta^{14}C_{oth} = \Delta^{14}C$ from other sources

$\Delta^{14}C_{ff}$ = -1000 ‰

Since CO_{2mes} is unknown for the plant samples, it can be substituted from Eqs. (2) to (3) (Turnbull et al., 2009) and we get following expression for CO_{2ff}

$$CO_{2ff} = \frac{CO_{2bg}\left(\Delta^{14}C_{mes} - \Delta^{14}C_{bg}\right)}{\Delta^{14}C_{ff} - \Delta^{14}C_{mes}} - \frac{CO_{2oth}\left(\Delta^{14}C_{other} - \Delta^{14}C_{mes}\right)}{\Delta^{14}C_{ff} - \Delta^{14}C_{mes}} \quad (4)$$

All the sampling sites are far from nuclear power plants and oceans. So, second term in above expression is a correction due to heterotopic respiration only. If we consider this correction also as zero, it will introduce an error of ~0.2 to 0.3 ppm during the winter season and ~0.4 to 0.8 ppm during the summer season in CO_{2ff} values (Turnbull et al., 2006, 2009).

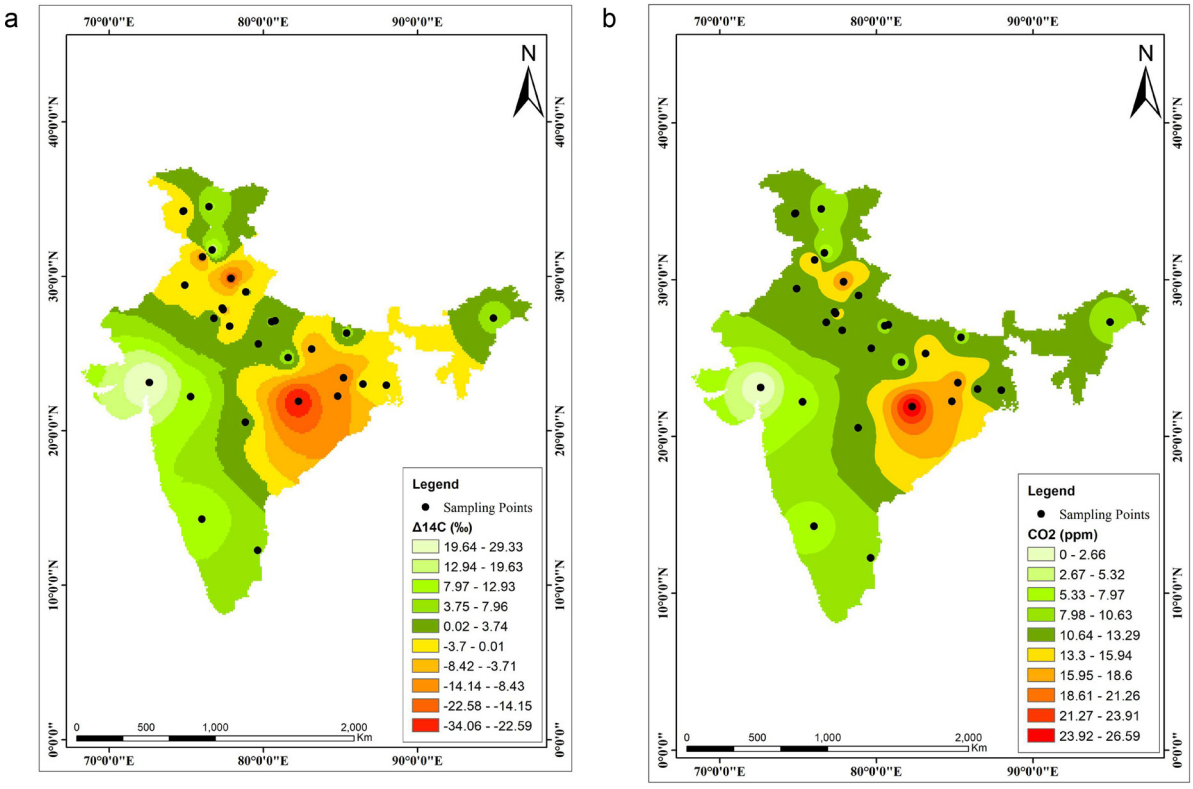

Fig. 1 – (a) Spatial distribution of $\Delta^{14}C$ for the year 2017 across India. (b) spatial distribution of CO_{2ff} for the year 2017 across India. Geostatistical Analyst tools in ESRI's ArcMap software were used for mapping. An Inverse Distance Weighted (IDW) method was used as an interpolation method.

Therefore, CO_{2ff} can be calculated using following simplified expression

$$CO_{2ff} = \frac{CO_{2bg}\left(\Delta^{14}C_{mes} - \Delta^{14}C_{bg}\right)}{\Delta^{14}C_{ff} - \Delta^{14}C_{mes}} \quad (5)$$

2. Results and discussion

2.1. *Spatial distribution of $\Delta^{14}C$ over India*

We have determined the $\Delta^{14}C$ values using Eq. (1) for all the samples collected during the three-year time period (2017, 2018 and 2020) and analyzed values are given in supporting material. To determine the spatial distribution map of $\Delta^{14}C$ over India, we have chosen the year 2017 due to most of the samples collected during this year. Since background $\Delta^{14}C$ values at global background sites decreases at the average annual rate of 5‰ (Graven et al., 2012), we have also scale down $\Delta^{14}C$ values of the samples collected for the years 2018 and 2020 to the year 2017 by the rate of 5‰ per year. Similar approach is also followed by Santos et al. (2019) for producing a $\Delta^{14}C$ distribution over the Rio de Janeiro state, Brazil. Based on this approach these values are adjusted for $\Delta^{14}C$ and given in supplementary data. We have also presented the spatial distribution map of $\Delta^{14}C$ in Fig. 1a. Since we have collected full plant samples from some locations, we have measured different plant organs in these samples. For calculating a single $\Delta^{14}C$ value from such locations, we have considered the average of all $\Delta^{14}C$ values of these organs from the same plants. Similarly for the multiple samples of different crop plants from a single location, we have calculated the average value of $\Delta^{14}C$ values from all the plants from that particular location.

All the samples collected for all these years 2017, 2018 and 2020 are reflecting the $\Delta^{14}C$ signal of winter season except samples from three sites that are reflecting signals of summer season. From those three sites, type of samples collected and their grown period are as following: Rice plants samples collected in August 2017 from Nischintpur, West Bengal (Grown period: June 2017 to August 2017), wild strawberries leaves collected in July 2017 from a site at an elevation of 3220 m from Jammu and Kashmir (Grown period: March 2017 to July 2017), Barley grains collected in July 2020 from a location from Kargil, Ladakh (Grown period: March 2020 to July 2020).

Results show that the $\Delta^{14}C$ values for the year 2017 are varying between 29.33‰ to -34.06‰ across India where the highest value belongs to a location from Gujarat, while lowest value belongs to a location from Chhattisgarh. Other lower values of $\Delta^{14}C$ are observed over Roorkee (Uttarakhand), Jharkhand, Orissa, Punjab, Mathura and Chandauli (both from Uttar Pradesh), respectively. In addition to the above, samples were also collected from four high altitude sites (elevations of 3220 m, 3197 m, 1626 m and 1170 m) as shown in supplementary data. $\Delta^{14}C$ values for these sites are -6.83‰, 3.46‰, 8.88‰ and 17.18‰, respectively. It is also interesting to note that one of these sites (having an elevation of 3220 m) is more depleted

in $\Delta^{14}C$ while this site is located in the forest area. However, it is indicating that the transport of fossil fuel CO_2 from nearby urban locations might be one of the reasons for the depletion. Further, we have also measured radiocarbon in pine tree leaves from this location and corresponding $\Delta^{14}C$ value was observed as 9.07‰ that is higher than the value observed in strawberry leaves (-6.83‰). Pine tree leaves (being a perennial tree) are showing a signal of long-term atmospheric CO_2 while strawberry leaves are showing a signal of short-term atmospheric CO_2 that may be affected by transport of recent CO_2 from nearby urban areas. $\Delta^{14}C$ values from other sites from Rajasthan, Haryana, Uttar Pradesh, Bihar, West Bengal, Assam, Maharashtra and Madhya Pradesh are varying between -1.08‰ and 12.92‰ while $\Delta^{14}C$ values from Karnataka and Tamil Nadu, parts of southern India are observed as 12.36‰ and 6.30‰, respectively.

2.2. *Selection of background value*

As it is reported in Turnbull et al. (2009) that the calculation of CO_{2ff} mole fractions is affected by the selection of background site. We do not have samples from a proper background site in this study. Since we have observed the highest $\Delta^{14}C$ value (29.33 ‰) in this study from a rural site from Gujarat for a wheat plant stem sample collected in 2017 as described earlier. Therefore, we have considered this value as $\Delta^{14}C_{bg}$ for calculation of CO_{2ff} mole fraction values for this study. This background value ($\Delta^{14}C_{bg}$) is higher than the other contemporary background values in the northern hemisphere (Hammer and Levin, 2017; Wang et al., 2021) but matching within the range of the background value used by Dasari et al. (2020). They have estimated $\Delta^{14}C$ value of fresh biomass (annual plants) as 20% ± 10‰ for the South Asian region for the year 2016. Sample whose $\Delta^{14}C$ value is considered as background in this study is also showing signature of CO_2 from the years 2016 and 2017 both because it is grown between November 2016 and April 2017.

Background CO_2 values (CO_{2bg}) have been taken from Mauna Loa Atmospheric Baseline Observatory located in Hawaii, United States (Keeling et al., 2005). We have used the mean value of atmospheric CO_2 for different months according to the growing season of crop plants as background CO_2 value. For example, most of our samples are collected in the month of April 2017, we have taken the average of six-month CO_2 values from November 2016 to April 2017 from this record and used it (406.15 ppm) as CO_{2bg} value. CO_{2bg} values used for other samples are given in supplementary data. An error of 5 ppm because of the choice of CO_{2bg} value from this site will result in the maximum error of 0.33 ppm in our CO_{2ff} values that is smaller than the error induced by radiocarbon measurement uncertainty.

2.3. *Spatial distribution of CO_{2ff} over India*

It is also emphasizing that understanding the role of the fossil fuel CO_2 is one of the prime concerns in terms of estimating its contribution towards the total atmospheric CO_2. In this section we have discussed the spatial distribution of fossil fuel derived CO_2 across India for the year 2017 as shown in Fig. 1b and corresponding values are given in supplementary data. An uncertainty value of 1.55 ppm in CO_{2ff} is estimated from the external uncertainty of 3.71‰ in radiocarbon measurements.

Crop plants develop their biomass by absorbing CO_2 from the atmosphere during photosynthesis process in a well-developed planetary boundary layer (Hsueh et al., 2007). Therefore, both $\Delta^{14}C$ and CO_{2ff} in the present study represent time integrated CO_2 signals of daytime only. Since CO_{2ff} values are directly depending upon the $\Delta^{14}C$ values, therefore, CO_{2ff} values are following the same pattern to that of $\Delta^{14}C$ values. Further it can be noticed that the higher CO_{2ff} values coincides with the depleted values of $\Delta^{14}C$ and vice versa. Highest CO_{2ff} value is from a location from Chhattisgarh where CO_{2ff} value is found to be 26.59 ppm. Since we have considered a location from Gujarat as a background location for calculation of CO_{2ff}, this location shows a minimum CO_{2ff} emission and all other CO_{2ff} values are calculated relative to this location. CO_{2ff} values from four high elevation locations are varying from 4.85 ppm to 14.87 ppm. In addition, we also found higher CO_{2ff} emission values from Roorkee (Uttarakhand), Jharkhand, Orissa, Punjab, Mathura and Chandauli (both from Uttar Pradesh) where CO_{2ff} values are ranging from 19.53 ppm to 15.35 ppm, respectively. CO_{2ff} values from other sampling sites in India are found to be varied between 6.58 ppm to 12.37 ppm.

Among all sampling sites having high CO_{2ff} values, two sample sites (Roorkee and Mathura) are heavily affected by high fossil fuel emission from vehicular traffic. In an earlier study it is reported that plants near highways are enriched by a factor up to 13% in fossil fuel carbon (Lichtfouse et al., 2005). While the other three sampling sites showing high CO_{2ff} values are from Chhattisgarh, Orissa and Jharkhand. These high CO_{2ff} values are expected because these three states have the highest coal reserve in India (Coal reserve in India, Ministry of Coal 18th October, 2021) http://coal.nic.in/major-statistics/coal-reserves and also highest CO_2 emission regions from coal based thermal power plants (Sahu et al., 2017).

It is also reported that most of the sampling sites are located in rural areas for the present study. Agricultural activities such as tillage, seeding, weed management and irrigation in rural areas are mechanized and these machines (tractors, diesel based pumps for irrigation etc.) use fossil fuels for their operations (Sinha et al., 2020). Results in this study may also be affected by the local CO_2 emitted by these machines.

Out of 29 sampling locations in this study, 14 sites (sampling sites from Punjab, Haryana, Uttar Pradesh, Rajasthan, Bihar and West Bengal) are located in the Indo-Gangetic Plain (IGP). IGP is highly polluted and dominated by the aerosols and frequent haze episodes especially in winter due to the influence of emission sources such as anthropogenic, agriculture residue burning, domestic fire etc. (Bikkina et al., 2019; Singh et al., 2018; Kumar et al., 2018). Also, we presented the analysis of CO_{2ff} values during the winter season. This study presents the first of its kind observations of CO_{2ff} mole fractions from large number of sampling sites (14 locations) of the IGP region. CO_{2ff} values of all the locations within IGP are ranging from 9.95 ppm to 19.53 ppm. We have presented a comparison of $\Delta^{14}C$ values and CO_{2ff} mole fractions from similar studies carried out over different countries in Table 1.

Table 1 – A comparison of the results from similar studies around the world.

S. No.	Country	Study Period	Sampling Plant	$\Delta^{14}C$ (‰)	Maximum CO_{2ff} (ppm)	Reference
1.	USA	Summer 2004 (May – September)	Corn leaves	37.2 to 68.9	–	Hsueh et al., 2007
2.	China	Summer 2010 (May – September)	Corn leaves	-4.3 to 39.2	16.09	Xi et al., 2013
3.	South Korea	2010, 2011, 2012, 2013 (April – June)	Ginkgo leaves	2010: -111.8 to 36.1, 2011: -97.9 to 35.6, 2012: -116.3 to 35.6, 2013: -123 to 35,	–	Park et al., 2013, 2015
4.	The Netherlands, France and western Germany	2010 - 2012	Corn leaves	The Netherlands (2010-2012): 15.82 to 38.07, France (2012): 19.64 to 43.28, Germany (2012): 10.16 to 24.7	–	Bozhinova et al., 2016
5.	India	2017 (Rabi season: Oct/Nov 2016–March/April 2017)	Wheat (leaves, stem, grains), Mustard (leaves, grains), Rice (leaves, grains)	-34.06 to 29.33	26.59	Present Study

2.4. *Effect of sampling different plant organs on $\Delta^{14}C$ and CO_{2ff}*

As described earlier, we have collected different plant organs (leaves, grain, stem) depending upon the availability. Different parts of crop plants are developed at different time periods during their growth (Bozhinova et al., 2013). If we measure $\Delta^{14}C$ for different plants organs, they provide signatures of CO_2 absorbed during their growth period. Therefore, $\Delta^{14}C$ values of different plant organs may be different and this may induce some error in CO_{2ff} estimations. To study the effect of sampling different plant parts on the CO_{2ff} estimations, we have measured $\Delta^{14}C$ values in grains and leaves from a single matured crop plant. Total 9 such pairs of samples (leaves and grains) were collected from 9 plants (8 wheat plants and 1 mustard plant) over 8 locations. Out of these 9 pairs, two pairs of samples were collected in two consecutive years (2017 and 2018) from a single location (Dholpur, Rajasthan, location code: Raj_Dho). From this location in the year 2017, an additional sample of stem was also collected with leaves and grains from the same wheat plant. The details of the sampled plant, sampled plant organs, measured $\Delta^{14}C$ values with one sigma uncertainties, difference in $\Delta^{14}C$ values of different plant organs is given in Table 2.

Our analysis shows that the difference between $\Delta^{14}C$ values of grains and leaves is varying from 0.38‰ to 13.88‰ except from one location (village - Alampur, Post – Sankh, Dist.-Hardoi, UP) where the difference is observed as 33.52‰. This large difference may be an artifact of the local source of modern CO_2 over particular location. Since the grains in cereal crops are developed partly from the biomass reallocated from other parts of the plant while partly from freshly assimilated CO_2 from the atmosphere (Bozhinova et al., 2013). Generally other crops are also grown with wheat crops in nearby fields. Some of these crops (such as potato, mustard etc.) are harvested when grains of wheat start growing. At some places, crop residues are burnt post harvesting, and this burning may be the source of modern CO_2. This CO_2 is absorbed by growing grains and reflected in higher $\Delta^{14}C$ values of grains. If we assume this sample as outlier, then the mean difference between leaves and stem is 5.50‰ with the standard deviation of 4.89‰ that is slightly higher than the reported value (4.8‰) in Europe for similar study (Bozhinova et al., 2013). This difference in $\Delta^{14}C$ values may induce an error of maximum 2.30 ppm in our CO_{2ff} calculation in this study that is higher than the external uncertainty (1.55 ppm).

The difference between stem and grain is 1.49‰ while between leave and stem is 7.61‰ over Dholpur, Rajasthan location. Larger difference between leaves and stem is expected because of the difference of one month between growing of stems and leaves (Bozhinova et al., 2013). Although a larger number of stem samples are required to fully understand the effect of its sampling on the $\Delta^{14}C$ and CO_{2ff} in place of leave and grain. Difference between stem and grains may induce an error of 0.62 ppm while difference between stem and leaves may induce an error of 3.18 ppm in CO_{2ff} values. It is also interesting to note that the $\Delta^{14}C$ values of grains in wheat plant are greater than the $\Delta^{14}C$ values of leaves for six pairs of samples except two pair of samples where this value is lesser by small amounts (0.38‰ and 1.06‰, respectively) from the above analysis. One of the possible reasons for this interesting result may be the effect of regional biomass burning. Because biomass burning peaks during the summer months (March-May) for most of the Indian states (Sahu et al., 2015). Grain filling stage in the wheat crop plants also starts in the month of March. Therefore, $\Delta^{14}C$ values of grains are affected by modern CO_2 produced by biomass burning and resulted in the higher $\Delta^{14}C$ value in comparison to leaves.

Table 2 – $\Delta^{14}C$ values of different plant organs from 8 locations.

S. No.	Location Code*, Sampled Plant	Sampled Plant Organ	$\Delta^{14}C$ (‰)	Uncertainty	Difference in $\Delta^{14}C$ (‰) values		
					Grains - Leaves	Stem - Grains	Stem - Leaves
1.	UP_VAR, Wheat	Grains	-13.33	2.21	0.38		
		Leaves	-12.95	2.38			
2.	UP_HAMIR, Wheat	Grains	18.32	2.29	33.52		
		Leave	-15.20	2.65			
3.	HAR_SIR, Wheat	Grains	3.74	2.40	7.42		
		Leaves	-3.68	2.61			
4.	UP_HAR, Wheat	Grains	9.42	2.23	13.88		
		Leaves	-4.46	2.73			
5.	UP_UNN, Wheat	Grains	6.20	2.28	2.94		
		Leaves	3.26	2.30			
6.	RAJ_DHO_01/04/2018#, Wheat	Grains	1.16	2.15	1.06		
		Leaves	2.22	2.40			
7.	RAJ_DHO_2017, Wheat	Grains	3.50	2.35	6.12	1.49	7.61
		Leaves	-2.62	2.79			
		Stem	-4.11	2.72			
8.	ASSAM_MOR, Mustard	Grains	8.28	2.41	11.74		
		Leaves	-3.46	2.30			
9.	Raj_ALW, Wheat	Grains	4.40	2.45	0.47		
		Leaves	3.93	2.59			
Mean and standard deviation of all the differences in $\Delta^{14}C$ (‰) values of grains and leave excluding second location					5.50 and 4.89		

* Detailed information of these location codes given in the supplementary data.
\# To differentiate samples from two consecutive years from same location, date of collection is added in the location code.

2.5. *Effect of sampling different crop plants grown in same season*

As described in Section 2.1, we have collected crop plants other than wheat such as mustard, rice and barley if we could not get wheat plants from same locations for this study. In this section, we have assessed the effect of sampling different crop plants grown in the same season on $\Delta^{14}C$ and CO_{2ff} values. To assess the effect, we have collected various crop plants grown in the same season with wheat plants from two locations (Dholpur, Rajasthan and Moran, Assam). From a rural location in Dholpur, Rajasthan, samples were collected from two different crop plants, wheat and mustard, for all three years 2017, 2018 and 2020 while potato was also collected with wheat and mustard plants in the year 2018. Samples collected in 2017 and 2018 are grown in the same season starting from November 2017 and ending in April 2018. In 2017, wheat leaves (one month 15 days old crop) and mustard leaves (two months five days old crop) were collected on 25th December 2017. In 2018, wheat leaves (three months old crop) and mustard leaves (three months twenty days old crop) were collected on 10th February 2018. Potato was also collected on this date, just 15 days before it's harvesting. All these plants are grown in adjacent fields from the same location. Sowing time of these crops was in following order: mustard, potato after five days of mustard, wheat after 20 days of mustard. In 2020, samples were collected at a distance of 2 km from the previous location in the month of March at the flowering of wheat and maturity of mustard. $\Delta^{14}C$ values with one-sigma uncertainties of all the plants from this location (Raj_DHO) have been shown in Table 3. In 2017, the difference between $\Delta^{14}C$ values from wheat and mustard plant is 3.03‰ while in 2020, this difference is 1.98‰. In 2018, the difference observed in $\Delta^{14}C$ values between wheat and mustard plant is 6.61‰ while difference between wheat and potato plant is 8.13‰ and difference between potato and mustard plant is 1.52‰. Mean difference in $\Delta^{14}C$ values between wheat and mustard plant is 3.87‰ with 1.98‰ standard deviation while mean difference in $\Delta^{14}C$ values for all three plants from this location is 4.25‰ with standard deviation of 2.63‰. The mean difference between mustard and wheat plant from the same location is comparable to external uncertainty in radiocarbon measurements and the difference between all plants is slightly higher than the external uncertainty. Sampling of wheat and mustard plant can show an error of 1.62 ppm in CO_{2ff} values while sampling of all three plants can induce an error of 1.78 ppm in CO_{2ff} values.

We have sampled four different types of plants from another location in Assam for the year 2017. These four types of plants were wheat, rice, bhut (chili) and mustard. These plants are sown in between 20 and 30 days (exact days are not known) in nearby fields (not adjacent) from this location. $\Delta^{14}C$ values with one-sigma uncertainties of all the plants from this location (ASSAM_MOR) have also been shown in Table 3. Here we have observed large differences in $\Delta^{14}C$ values of these plants. Maximum difference of 36.05‰ is observed between wheat and rice plant while minimum difference of 1.99‰ is observed between mustard and chili plants. Difference between mustard and wheat plant is 24.06‰. Mean difference in $\Delta^{14}C$ values for all plants is 18.35‰ with standard deviation of 11.42‰ from this location. This difference can induce a larger error of 7.68 ppm in CO_{2ff} values in our study. We observed different behavior of crop plants in terms of $\Delta^{14}C$ values from these two locations. For one location this difference from different crop plants is slightly higher than the external uncertainty

Table 3 – $\Delta^{14}C$ values of different plants grown in same season.

S. No.	Location Code	Year of sampling	Sampled plant	$\Delta^{14}C$ (‰)	Uncertainty	Difference in $\Delta^{14}C$ (‰) values			
						Wheat - Mustard		All Plants	
						Mean	SD	Mean	SD
1.	RAJ_DHO	2017	Wheat	-8.66	2.47	3.87	1.98	4.25	2.63
			Mustard	-11.69	2.27				
		2018	Wheat	-17.58	2.84				
			Mustard	-10.97	2.73				
			Potato	-9.45	2.25				
		2020	Wheat	-27.81	1.68				
			Mustard	-25.83	1.74				
2.	ASSAM_MOR	2017	Wheat	26.47	2.46	24.06	-	18.35	11.42
			Rice	-9.57	2.29				
			Bhut (Chili)	0.43	2.19				
			Mustard	2.41	2.36				

while this difference is larger from other location. This different behavior of sampling different plants on $\Delta^{14}C$ values at two different sampling locations can be attributed to the local sources, environmental and climatic conditions. It is also important to note that results from Dholpur, Rajasthan are based on the samples from three years while results from Assam are based on samples from a single year only. It is also suggesting that more samples from more locations can provide robust insights in this aspect.

2.6. *Annual and intra seasonal variations in $\Delta^{14}C$ and CO_{2ff} values*

In this section, we focus on understanding the annual variations of $\Delta^{14}C$ and CO_{2ff} over a single location. In order to explore these annual variations, we have collected samples of wheat plants in 2017, 2018 and 2020 from a rural village in Dholpur, Rajastan. Samples in the years 2017 and 2018 were collected from adjacent fields in the month of April at maturity, while in the year 2020, samples were collected in the month of March at the flowering stage of wheat. Location of the field of samples collected in 2020 was 2 km away from the location of samples collected in 2017 and 2018. These samples will show $\Delta^{14}C$ and CO_{2ff} values of their growing period i.e., from November 2016 to April 2017 for 2017, from November 2017 to March 2018 for 2018, November 2019 to February 2020 for 2020, respectively. In the year 2017, we have collected leaves, stem and grains of wheat while in the year 2018, we have collected leaves and grains of wheat. Sampling locations were situated at more than 500 m distances from the road and more than 1 km distance from the adjacent villages. All tube wells used for irrigation in the adjacent areas are electric motor based.

We have presented the $\Delta^{14}C$ and CO_{2ff} values for all the years shown in Fig. 2a and b, respectively and taken the average of $\Delta^{14}C$ values of all plant organs (leaves, grain and stem) to find out the $\Delta^{14}C$ value for the year 2017 and 2018. Observed $\Delta^{14}C$ values are -1.08‰ and 1.69‰ for the years 2017 and 2018, respectively while $\Delta^{14}C$ value is -25.83‰ in the year 2020. There is an increase of 2.77‰ in the year 2018 but at a distance of 2 km, there is a large decrease of 27.52‰ in the year 2020. To calculate corresponding CO_{2ff} mole fraction values using Eq. (5), we have first calculated background $\Delta^{14}C$ values for the year 2018 and 2020 from the background $\Delta^{14}C$ value of 2017 (29.33‰) after considering the annual average decrease rate of 5‰ (Graven et al., 2012). Therefore, background $\Delta^{14}C$ values for the year 2018 and 2020 are 24.33‰ and 14.33‰, respectively. CO_{2bg} values are taken as 407.51 ppm and 412.40 ppm as mean values for the corresponding growing months of plant samples for the year 2018 and 2020, respectively from the CO_2 observation record available from Mauna Loa, United States (Keeling et al., 2005). The corresponding CO_{2ff} values for this location are observed as 12.37, 9.21 and 17.00 ppm for the years 2017, 2018 and 2020, respectively as shown in Fig. 2b. It can clearly be seen that these results show less annual variation in $\Delta^{14}C$ and CO_{2ff} values over the period of two years from the same location, however large variations have been observed with distance of 2 km in the third year. Since there is no major fossil fuel source at a distance of 2 km, it means there may be large change in fossil fuel emission activities in the vicinity of this location between the years 2018 and 2020.

In addition to the annual variations, we have further focused on addressing the changes in $\Delta^{14}C$ and CO_{2ff} values during different growing stages of plants in single crop season. In order to address this, we have collected samples of these plants (Wheat and Mustard) from the same location (Dholpur, Rajathan) described in the last section. Wheat leaves were collected on 25th December 2017 (one month 15 days old crop, tillering), 10th February 2018 (three months old crop, flowering) and 1st April 2018 (mature plants, collected seed and leaves both, 10 days before the harvesting) from same field. Similarly mustard leaves were collected on 25th December 2017 (two months five days old crop, at pod formation) and 10th February 2018 (three months 20 days old crop, at maturity) from the same field. Both of these wheat and mustard fields are situated adjacent to each other.

We have shown the $\Delta^{14}C$ and CO_{2ff} values in Fig. 3a and b, respectively. $\Delta^{14}C$ values for wheat leaves samples collected on 25th Dec 2017, 10th Feb 2018 and 1st April 2018 are -8.66‰, -17.58‰ and 2.22‰, respectively. Similarly, $\Delta^{14}C$ values for mustard leaves samples collected on 25th Dec 2017 and 10th Feb 2018 are -11.69‰ and -10.97‰, respectively. The corre-

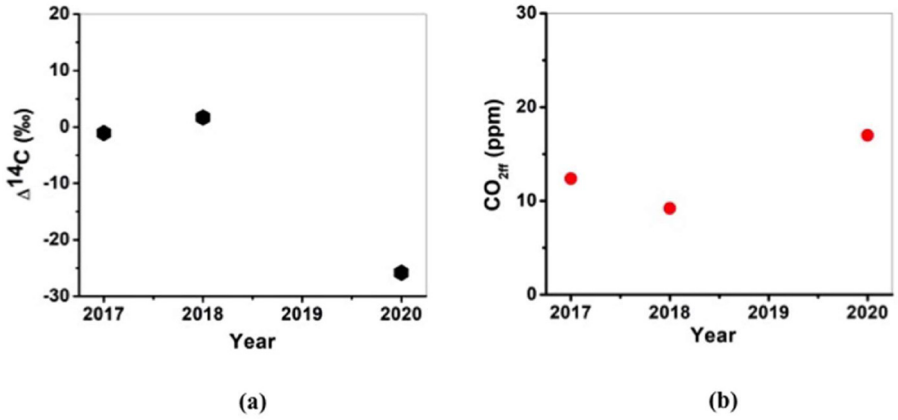

Fig. 2 – (a) Variation in $\Delta^{14}C$ values for the study period from single location (Dholpur, Rajasthan) (b) Corresponding variations in CO_{2ff} mole fractions from the same location.

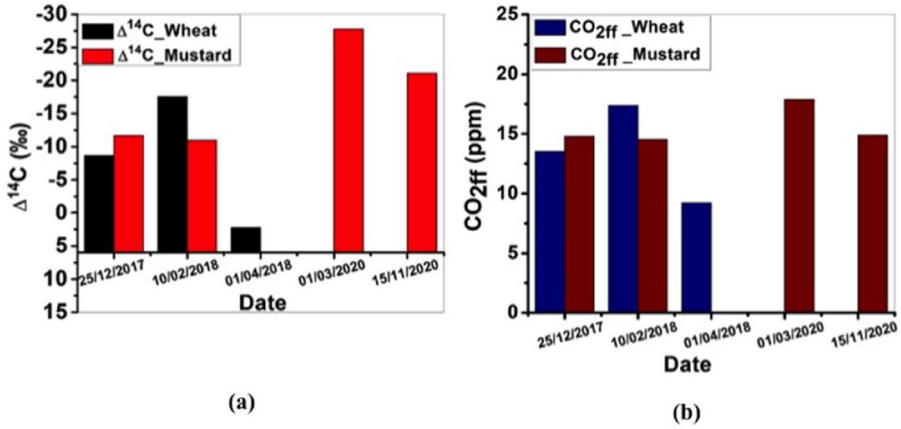

Fig. 3 – (a) $\Delta^{14}C$ values of wheat and mustard samples on different growing stages from single season (b) Corresponding CO_{2ff} values with their sampling dates.

sponding CO_{2ff} values observed for wheat samples are 13.51, 17.36 and 9.21 ppm, respectively and corresponding CO_{2ff} values observed for mustard samples are 14.80 and 14.53 ppm, respectively. There are large variations in $\Delta^{14}C$ and CO_{2ff} values for wheat samples at its different growing stages in a season while these values are relatively constant for mustard samples in the same season from the same location. At a distance of 2 km, mustard grains and leaves samples were collected from another location on 01st March 2020 (at maturity) and 15th Nov 2020 (one month old crop), respectively. Samples collected on 01st March 2020 are showing $\Delta^{14}C$ and CO_{2ff} values of the period from October 2019 to February 2020 while another sample is showing these values for the period of one month from 15th October 2020 to 15th November 2020. $\Delta^{14}C$ values for these samples were -27.81‰ and -21.07‰ respectively (as shown in Fig. 3a). Corresponding CO_{2ff} values for these samples are 17.88 and 14.87 ppm, respectively (as shown in Fig. 3b). During the period of eight months, there is a decrease of 6.74‰ in the $\Delta^{14}C$ value in this region. It can be observed from these results that crop plants can also be utilized to examine CO_{2ff} values for shorter time periods too.

3. Summary and conclusions

As the recent rise in the fossil fuel emissions over different parts of the world especially for the developing countries like India results in the increase in the atmospheric CO_2 concentrations. However, the studies to examine the exact quantification and contribution of the fossil fuel derived CO_2 towards total CO_2 is still elusive due to sparseness of observational and tracer-based studies over India region. In the present study we have used the radiocarbon measurements to address the spatial distribution of $\Delta^{14}C$ and fossil fuel derived CO_2 based on the crop plant samples across India.

The findings based on radiocarbon measurements over India distilled from this study are as follows:

- Results show that the $\Delta^{14}C$ values in the year 2017 are varying between 29.33‰ and -34.06‰ across India, while CO_{2ff} values are ranging from 4.85 ppm to 26.59 ppm across India.

- Higher CO_{2ff} values are obtained for the sites either from highest coal reserve area (Chhattisgarh, Orissa and Jharkhand) or from the roadside sites.
- Effect of sampling different plant organs on $\Delta^{14}C$ and CO_{2ff} is addressed and found that the sampling of grain in place of leave (in wheat and mustard plants) can induce a difference of 2.30 ppm in CO_{2ff} values while 5.50‰ in $\Delta^{14}C$ that is larger than the measurement error in this study.
- Similarly, effect of sampling different crop plants from the same season on $\Delta^{14}C$ and CO_{2ff} is also assessed. An error of 1.76 ppm in CO_{2ff} values corresponding to the error of 4.25‰ in $\Delta^{14}C$ values is observed for the samples collected from Dholpur, (Rajasthan) which is slightly higher than the measurement error in this study. The error in CO_{2ff} value is found to be quite higher of about 7.68 ppm corresponding to 18.25‰ over a sampling location in Assam.
- The annual and intra-seasonal variations of $\Delta^{14}C$ and CO_{2ff} values from a single location (Dholpur, Rajasthan) are also studied. In the year 2018, there is an increase of 2.77‰ while large decrease of 27.52‰ is observed in the year 2020. Large fluctuations in $\Delta^{14}C$ and CO_{2ff} are observed at different growing stages of wheat samples while these variations are found to be relatively constant for mustard samples.

From our study it is concluded that the regional pattern of $\Delta^{14}C$ and CO_{2ff} are affected by regional fossil fuel sources and ^{14}C in crop plants can effectively be used to trace these sources. However, same plant organ and same crop plant should be used for sampling to avoid error in the results. The present study provides a CO_{2ff} database across India that can be utilized by other researchers, policy makers for the mitigation policies.

Acknowledgements

Authors are thankful to Ministry of Earth Science (MoES), Govt. of India for providing financial support (reference numbers: MoES/16/07/11 (i)-RDEAS and MoES/P.O.(Seismic) 8(09)-Geochron/2012) to establish AMS facility at IUAC, New Delhi. Authors would like to acknowledge the support of colleagues, collaborators and friends for collecting the samples. Authors also acknowledge the support from Mr. Sreerama Naik S R, SRF, JNU, New Delhi for the mapping using ESRI's ArcMap software. We thank the anonymous reviewers for their suggestions and constructive comments on our manuscript.

Appendix A Supplementary data

Supplementary material associated with this article can be found, in the online version, at doi:10.1016/j.jes.2021.11.003.

REFERENCES

Andres, R.J., Boden, T.A., Bréon, F.-M., Ciais, P., Davis, S., Erickson, D., et al., 2012. A synthesis of carbon dioxide emissions from fossil-fuel combustion. Biogeosciences 9, 1845–1871.

Bikkina, S., Andersson, A., Kirillova, E.N., Holmstrand, H., Tiwari, S., Srivastva, A.K., et al., 2019. Air quality in megacity Delhi affected by countryside biomass burning. Nat. Sustain. 2, 200–205.

Boesch, H., Baker, D., Connor, B., Crisp, D., Miller, C., 2011. Global characterization of CO_2 column retrievals from shortwave-infrared satellite observations of the orbiting carbon observatory-2 mission. Remote Sens. 3 (2), 270–304.

Bozhinova, D., Combe, M., Palstra, S.W.L., Meijer, H.A.J., Krol, M.C., Peters, W., 2013. The importance of crop growth modeling to interpret the $\Delta^{14}CO_2$ signature of annual plants. Glob. Biogeochem. Cycles 27, 792–803.

Bozhinova, D., Palstra, S., Van der Molen, M., Krol, M., Meijer, H., Peters, W., 2016. Three years of $\Delta^{14}CO_2$ observations from maize leaves in the Netherlands and western Europe. Radiocarbon 58 (3), 459–478.

Ciais, P., Sabine, C., Bala, G., Bopp, L., Brovkin, V., Canadell, J., et al., 2013. Car-bon and other biogeochem. Cy. In: Stocker, T.F., Qin, D., Plattner, G.-K., et al. (Eds.), Climate Change 2013: the Physical Science Basis. Contribution of Working Group I to the Fifth Assessment Report of the Intergovernmental Panel on Climate Change. Cambridge University Press, Cambridge, United Kingdom and New York, NY, USA.

Chandra, N., Lal, S., Venkataramani, S., Patra, P.K., Sheel, V., 2016. Temporal variations of atmospheric CO_2 and CO at Ahmedabad in western India. Atmos. Chem. Phys. 16, 6153–6173.

Coal reserve in India, Ministry of Coal, Government of India. Available: http://coal.nic.in/major-statistics/coal-reserves. Accessed on 18th October, 2021.

Dasari, S., Andersson, A., Stohl, A., Evangeliou, N., Bikkina, S., Holmstrand, H., et al., 2020. Source quantification of south Asian black carbon aerosols with isotopes and modeling. Environ. Sci. Technol. 54, 11771–11779.

Directorate of Economics and Statistics (DES), 2015. Agricultural Statistics at a Glance 2014. Government of India, Oxford Univ. Press, New Delhi, India.

Friedlingstein, P., Jones, M.W., O'Sullivan, M., Andrew, R.M., Hauck, J., Peters, G.P., et al., 2019. Global carbon budget 2019. Earth Syst. Sci. Data 11, 1783–1838.

Ganesan, A.L., Chatterjee, A., Prinn, R.G., Harth, C.M., Salameh, P.K., Manning, A.J., et al., 2013. The variability of methane, nitrous oxide and sulfur hexafluoride in Northeast India. Atmos. Chem. Phys. 13, 10633–10644.

Graven, H.D., Guilderson, T.P., Keeling, R.F., 2012. Observations of radiocarbon in CO_2 at La Jolla, California, USA 1992–2007: analysis of the long term trend. J. Geophys. Res. 117, D02302.

Hammer, S., Levin, I., 2017. Monthly mean atmospheric $D^{14}CO_2$ at Jungfraujoch and Schauinsland from 1986 to 2016. Tellus B 65, 20092.

Hsueh, D.Y., Krakauer, N.Y., Randerson, J.T., Xu, X., Trumbore, S.E., Southon, J.R., 2007. Regional patterns of radiocarbon and fossil fuel-derived CO_2 in surface air across North America. Geophys. Res. Lett. 34, L02816.

Keeling, C.D., Piper, S.C., Bacastow, R.B., Wahlen, M., Whorf, T.P., Heimann, M., 2005. Atmospheric CO_2 and $^{13}CO_2$ exchange with the terrestrial biosphere and oceans from 1978 to 2000: observations and carbon cycle implications. In: Ehleringer, J.R., Cerling, T.E., Dearing, M.D. (Eds.), A History of Atmospheric CO_2 and its Effects on Plants, Animals, and Ecosystems. Springer Verlag, New York, pp. 83–113.

Kumar, M., Parmar, K.S., Kumar, D.B., Mhawish, A., Broday, D.M., Mall, R.K., et al., 2018. Long-term aerosol climatology over Indo-Gangetic Plain: Trend, prediction and potential source field. Atmos. Environ. 180, 37–50.

Kumar, K.R, Tiwari, Y.K., Valsala, V., Murtugudde, R., 2014. On understanding of land-ocean contrast of atmospheric CO_2

over Bay of Bengal: A case study during 2009 summer monsoon. Environ. Sci. Pollut. Res. 21, 5066–5075.
Kumar, R., Naja, M., Venkataramani, S., Wild, O., 2010. Variations in surface ozone at Nainital: a high-altitude site in the central Himalayas. J. Geophys. Res.-Atmos. 115, D16302.
Lal, S., Chandra, N., Venkataramani, S., 2015. A study of CO_2 and related trace gases using a laser-based technique at an urban site in western India. Curr. Sci. 109 (11), 2111–2116.
Le Quéré, C., Andres, R.J., Boden, T., Conway, T., Houghton, R.A., House, et al., 2013. The global carbon budget 1959–2011. Earth Syst. Sci. Data 5, 165–185.
Levin, I., Kromer, B., Schmidt, M., Sartorius, H., 2003. A novel approach for independent budgeting of fossil fuel CO_2 over Europe by $^{14}CO_2$ observations. Geo-phys. Res. Lett. 30, 2194.
Levin, I., Hesshaimer, V., 2000. Radiocarbon—A unique tracer of global carbon cycle dynamics. Radiocarbon 42, 69–80.
Lichtfouse, E., Lichtfouse, M., Kashgarian, M., Bol, R., 2005. ^{14}C of grasses as an indicator of fossil fuel CO_2 pollution. Environ. Chem. Lett. 3, 78–81.
Lin, X., Indira, N.K., Ramonet, M., Delmotte, M., Ciais, P., Bhatt, B.C., et al., 2015. Long-lived atmospheric trace gases measurements in flask samples from three stations in India. Atmos. Chem. Phys. 15, 9819–9849.
Marland, G., Boden, T.A., Andres, R.J., 2003. Global, Regional, and National CO2 Emissions in Trends: a Compendium of Data on Global Change, Carbon Dioxide Information Analysis Center. Oak Ridge National Laboratory, U.S. Department of Energy, Oak Ridge, TN.
Metya, A., Datye, A., Chakraborty, S., Tiwari, Y.K., Sarma, D., Bora, A., Gogoi, N., 2021. Diurnal and seasonal variability of CO_2 and CH_4 concentration in a semi-urban environment of western India. Sci. Rep.. 11, 2931.
Niu, Z, Zhou, W, Zhang, X, Wang, S, Zhang, D, Lu, X, et al., 2016. The spatial distribution of fossil fuel CO_2 traced by $\Delta^{14}C$ in the leaves of gingko (Ginkgo biloba L.) in Beijing City, China. Environ. Sci. Pollut. Res. Int. 23 (1), 556–562.
Park, J.H., Hong, W., Park, G., Sung, K.S., Lee, K.H., Kim, Y.E., et al., 2013. A comparison of distribution maps of $\Delta^{14}C$ in 2010 and 2011 in Korea. Radiocarbon 55 (2), 841–847.
Park, J.H., Hong, W., Xu, X., Park, G., Sung, K.S., Sung, K., et al., 2015. The distribution of $\Delta^{14}C$ in Koria from 2010 to 2013. Nucl. Instrum. Methods Phys. Res. Sect. B 361, 609–613.
Patra, P.K., Canadell, J.G., Houghton, R.A., Piao, S.L., Oh, N.-H., Ciais, P., et al., 2013. The carbon budget of South Asia. Biogeosciences 10, 513–527.
Prentice, I.C., Farquhar, G.D., Fasham, M.J.R., Goulden, M.L., Heimann, M, Jaramillo, V.J., Kheshgi, et al., 2001. The carbon cycle and atmospheric CO_2. In: Houghton, J.T., Ding, Y., Griggs, D.J. (Eds.), Climate Change 2000: the Science of Climate Change. Contributions of Working Group I to the Third Assessment Report of the Intergovernmental Panel on Climate Change. Cambridge University Press, pp. 183–237.
Randerson, J.T., Enting, I.G., Schuur, E.A.G., Caldeira, K., Fung, I.Y., 2002. Seasonal and latitudinal variability of troposphere D14CO2: Post bomb contributions from fossil fuels, oceans, the stratosphere, and the terrestrial biosphere, Global Biogeochem. Cycles 16 (4), 1112.
Sahu, S.K., Ohara, T., Beig, G., 2017. The role of coal technology in redefining India's climate change agents and other pollutants, Environ. Res. Lett. 12, 105006.
Sahu, L.K., Sheel, V., Pandey, K., Yadav, R., Saxena, P., Gunthe, S., 2015. Regional biomass burning trends in India: analysis of satellite fire data. J. Earth Syst. Sci. 124, 1377–1387.
Santos, G.M., Oliveira, F.M., Park, J., Sena, A.C.T., Chiquetto, J.B., Macario, K.D., et al., 2019. Assessment of the regional fossil fuel CO2 distribution through Δ14C patterns in ipê leaves: The case of Rio de Janeiro state, Brazil. City Environ. Interact. 1, 100001.
Sharma, R., Umapathy, G.R., Kumar, P., Ojha, S., Gargari, S., Joshi, R., et al., 2019. AMS and upcoming geochronology facility at Inter University Accelerator Centre (IUAC), New Delhi, India. Nucl. Instrum. Methods Phys. Res. Sect. B 438, 124–130.
Singh, N., Banerjee, T., Raju, M.P., Deboudt, K., Sorek-Hamer, M., Singh, R.S., et al., 2018. Aerosol chemistry, transport, and climatic implications during extreme biomass burning emissions over the Indo-Gangetic Plain. Atmos. Chem. Phys. 18, 14197–14215.
Sinha, R., Soni, P., Perret, S.R., 2020. Environmental and economic assessment of paddy based cropping systems in Middle Indo-Gangetic plains, India. Environ. Sustain. Indic. 8, 100067.
Stocker, T.F., Qin, D., Plattner, G.K., Tignor, M., Allen, S.K., Boschung, J., et al., 2013. IPCC, 2013: climate change 2013: the physical science basis. In: Contribution of Working Group I to the Fifth Assessment Report of the Intergovernmental Panel on Climate Change. Cambridge University Press, Cambridge, United Kingdom and New York, NY, USA, p. 1535. doi:10.1017/CBO9781107415324.
Stuiver, M., Polach, H.A., 1977. Discussion: reporting of 14C data. Radiocarbon 19, 355–363.
Suess, H.E., 1955. Radiocarbon concentration in modern wood. Science 122, 415.
Swathi, P.S., Indira, N.K., Rayner, P.J., Ramonet, M., Jagadheesha, D., Bhatt, B.C., et al., 2013. Robust inversion of carbon dioxide fluxes over temperate Eurasia in 2006–2008. Curr. Sci. 105, 201–208.
Tiwari, Y.K., Patra, P.K., Chevallieri, F., Francey, R.J., Krummel, P.B., Allison, C.E., et al., 2011. Carbon dioxide observations at Cape Rama, India for the period 1993–2002: implications for constraining Indian emissions. Curr. Sci. 101, 1562–1568.
Tiwari, Y.K., Revadekar, J.V., Ravi Kumar, K., 2013. Variations in atmospheric Carbon Dioxide and its association with rainfall and vegetation over India. Atmos. Environ. 68, 45–51.
Tiwari, Y.K., Vellore, R.K., Ravi Kumar, K., van der Schoot, M., Cho, C.H., 2014. Influence of monsoons on atmospheric CO_2 spatial variability and ground-based monitoring over India. Sci. Total Environ. 490, 570–578.
Trumbore, S.E., 2006. Carbon respired by terrestrial ecosystems—recent progress and challenges. Glob. Change Biol. 12, 141–153.
Turnbull, J.C., Miller, J.B., Lehman, S.J., Tans, P.P., Sparks, R.J., Southon, J., 2006. Comparison of $^{14}CO_2$, CO, and SF_6 as tracers for recently added fossil fuel CO_2 in the atmosphere and implications for biological CO_2 exchange. Geophys. Res. Lett. 33, L01817.
Turnbull, J.C., Lehman, S.J., Miller, J.B., Sparks, R.J., Southon, J.R., Tans, P.P., 2007. A new high precision$^{14}CO_2$ time series for North American continental air. J. Geophys. Res. 112, D11310.
Turnbull, J., Rayner, P., Miller, J., Naegler, T., Ciais, P., Cozic, A., 2009. On the use of $^{14}CO_2$ as a tracer for fossil fuel CO_2 Quantifying uncertainties using an atmospheric transport model. J. Geophys. Res. 114, D22302.
Turnbull, J.C., Graven, H., Krakauer, N.Y., 2016a. Radiocarbon in the atmosphere. In: Schuur, E., Druffel, E., Trumbore, S. (Eds.), Radiocarbon and Climate Change. Springer, Cham, pp. 83–137. doi:10.1007/978-3-319-25643-6_4.
Turnbull, J C, Keller, E D, Norris, M W, Wiltshire, R M, 2016b. Independent evaluation of point source fossil fuel CO_2 emissions to better than 10%. Proc. Natl. Acad. Sci. USA 113 (37), 10287–10291.
Turnbull, J.C., Mikaloff, F.S.E., Ansell, I., Brailsford, G.W., Moss, R.C., Norris, M.W., et al., 2017. Sixty years of radiocarbon dioxide measurements at Wellington, New Zealand: 1954–2014. Atmos. Chem. Phys. 17, 14771–14784.
Van de Wal, R.S.W., de Boer, B., Lourens, L.J., Köhler, P., Bintanja, R., 2011. Reconstruction of a continuous high-resolution CO_2 record over the past 20 million years. Clim. Past 7, 1459–1469.

Varga, T., Jull, A., Lisztes-Szabó, Z., Molnár, M., 2020. Spatial distribution of ^{14}C in tree leaves from Bali, Indonesia. Radiocarbon 62 (1), 235–242.

Wang, P., Zhou, W., Niu, Z., Xiong, X., Wu, S., Cheng, P., et al., 2021. Spatio-temporal variability of atmospheric CO_2 and its main causes: a case study in Xi'an city, China. Atmos. Res. 249, 105346.

Wenger, A., Pugsley, K., O'Doherty, S., Rigby, M., Manning, A.J., Lunt, M.F., et al., 2019. Atmospheric radiocarbon measurements to quantify CO_2 emissions in the UK from 2014 to 2015. Atmos. Chem. Phys. 19, 14057–14070.

WMO, 2020: WMO Greenhouse Gas Bulletin. Available: https://library.wmo.int/doc_num.php?explnum_id=10437. Accessed on 18th October 2021.

Xi, X.T., Ding, X.F., Fu, D.P., Zhou, L.P., Liu, K.X., 2013. $\Delta^{14}C$ level of annual plants and fossil fuel derived CO2 distribution across different regions of China. Nucl. Instrum. Methods Phys. Res. Sect. B 294, 515–519.